Journal of
Applied Remote Sensing

Monitoring oak-hickory forest change during an unprecedented red oak borer outbreak in the Ozark Mountains: 1990 to 2006

Joshua S. Jones
Jason A. Tullis
Laurel J. Haavik
James M. Guldin
Fred M. Stephen

Monitoring oak-hickory forest change during an unprecedented red oak borer outbreak in the Ozark Mountains: 1990 to 2006

Joshua S. Jones,[a] Jason A. Tullis,[b] Laurel J. Haavik,[a,c] James M. Guldin,[d] and Fred M. Stephen[a]

[a]University of Arkansas, Department of Entomology, Fayetteville, Arkansas 72701
jsjgis@gmail.com
[b]University of Arkansas, Department of Geosciences and Center for Advanced Spatial Technologies, Fayetteville, Arkansas 72701
[c]Great Lakes Forestry Centre, 1219 Queen Street East, Sault Ste. Marie, Ontario, P6A 2E5 Canada
[d]USDA Forest Service Southern Research Station, 100 Reserve Street, Hot Springs, Arkansas 71902

Abstract. Upland oak-hickory forests in Arkansas, Missouri, and Oklahoma experienced oak decline in the late 1990s and early 2000s during an unprecedented outbreak of a native beetle, the red oak borer (ROB), *Enaphalodes rufulus* (Haldeman). Although remote sensing supports frequent monitoring of continuously changing forests, comparable *in situ* observations are critical for developing an understanding of past and potential ROB damage in the Ozark Mountains. We categorized forest change using a normalized difference water index (NDWI) applied to multitemporal Landsat TM and ETM+ imagery (1990, 2001, and 2006). Levels of decline or growth were categorized using simple statistical thresholds of change in the NDWI over time. Corresponding decline and growth areas were then observed *in situ* where tree diameter, age, crown condition, and species composition were measured within variable radius plots. Using a machine learning decision tree classifier, remote sensing-derived decline and growth was characterized in terms of *in situ* observation. Plots with tree quadratic mean diameter at breast height ≥21.5 cm were categorized remotely as in severe decline. Landsat TM/ETM+-based NDWI derivatives reveal forest decline and regrowth in post-ROB outbreak surveys. Historical and future Landsat-based canopy change detection should be incorporated with existing landscape-based prediction of ROB hazard. [DOI: 10.1117/1.JRS.8.083687]

Keywords: change detection; Landsat TM/ETM+; normalized difference water index; *in situ* data; insect outbreak.

Paper 13131 received Apr. 26, 2013; revised manuscript received Oct. 29, 2013; accepted for publication Dec. 12, 2013; published online Jan. 23, 2014.

1 Introduction

In recent years (ca. 1995 to 2005), upland oak forests in Arkansas, Missouri, and Oklahoma experienced an episode of oak decline in concert with an unprecedented outbreak of the native longhorned beetle, the red oak borer (ROB), *Enaphalodes rufulus* (Haldeman) (Coleoptera: Cerambycidae). During this time, high ROB population levels were observed as contributing factors to the decline of multiple red oak species.[1–3] The ROB population densities began rising sharply from low populations in the late 1990s to peak in the early 2000s,[4] and then decreased from 2003 through 2007, returning to near-endemic densities.[5] When population densities remain consistent with native conditions, the ROB is not considered a pest.[6] However, during outbreak conditions, high population levels result in damage to the heartwood of oaks as numerous insects create galleries in the xylem of infested trees [Fig. 1(a)]. In addition, larval feeding in

0091-3286/2014/$25.00 © 2014 SPIE

recently formed xylem tissue weakens the host tree's ability to transport water and nutrients, resulting in crown dieback [Fig. 1(b)].[1,7,8]

The ROB is known to target only certain deciduous forest species. Northern red oak (*Quercus rubra* L.) is the principal host in Arkansas,[9] and experienced the greatest amounts of dieback and mortality, but other oak species also experienced mortality.[8,10,11] In general, red oak species (Section *Erythrobalanus*) were most affected, including black oak (*Quercus velutina* Lam.), southern red oak (*Quercus falcata* Michx.), and scarlet oak (*Quercus coccinea* Muenchh). Species of white oak (Section *Lepidobalanus*), including white oak (*Quercus alba* L.), post oak (*Quercus stellata* Wangenh.), and chestnut oak (*Quercus prinus* L.) were less affected.[1,8,12] The recent outbreak of the ROB resulted in various degrees of damage to at least 122,000 ha of oak forest within portions of the Ozark National Forest (ONF), with >75% mortality of mature oaks in heavily infested stands.[12] The occurrence and duration of this outbreak is unprecedented in recorded history.[6,13] It is valuable to develop and test simple, repeatable, and cost-effective methods for monitoring the ROB disturbance and its aftermath on a forest-wide scale.

1.1 *Landsat-Assisted Forest Monitoring*

Depending on the question of interest, the fundamental requirements of forest remote sensing may be high spatial resolution imagery with stereo capability[14] or airborne LiDAR (Ref. 15). This reflects a historical interest to complement purely *in situ* forest survey with aerial photography.[16,17] Nevertheless, relatively coarser spatial resolution remote sensing-assisted change detection has been successfully demonstrated for examining and quantifying meaningful forest canopy cover changes on a regular basis.[18] With the Landsat sensors providing the longest orbital record of forests at 30×30 m spatial resolutions (1982-present with relatively small gaps), this cost effective[19] monitoring legacy continues. Further, significantly improved spectral and radiometric properties inherent in Landsat 8 Operational Land Imager (OLI; launched February 11, 2013 and acquiring data since May 30, 2013), contribute to a bright future for this 30×30 m platform.[20]

1.2 *Vegetation Indices*

A normalized difference water index (NDWI) may be calculated using the near-infrared (NIR) and middle-infrared (MIR) portions of the electromagnetic spectrum.[21] Healthy tree leaves reflect most of the Sun's NIR radiation, and water stored in the cells of healthy vegetation absorb MIR radiation.[22] Because the NDWI is sensitive to the amount of leaf layers detected,[21,22] it may be useful for differentiating between full, healthy tree crowns and sparse, stressed crowns.

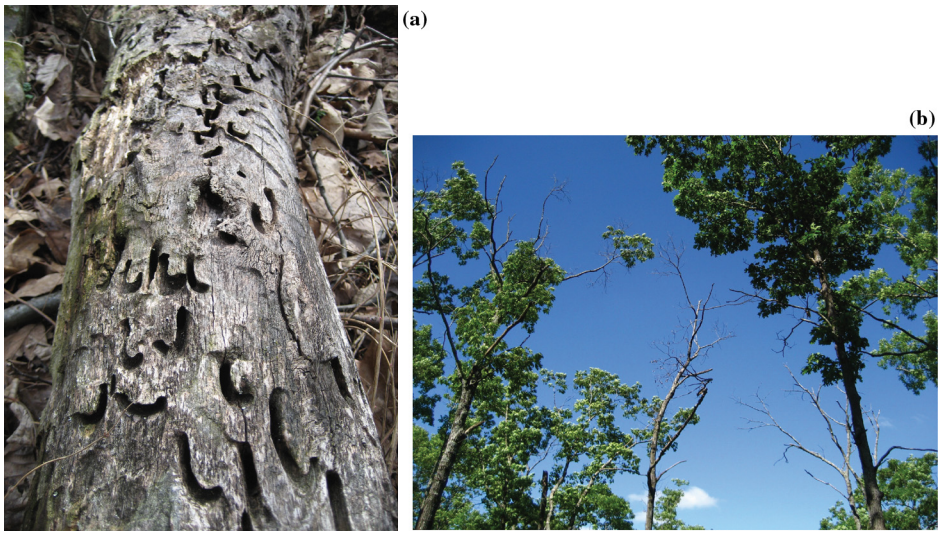

Fig. 1 (a) Old feeding tunnels exposed on a partially decomposed fallen dead *Quercus rubra* log, and (b) Crown dieback in a northern red oak canopy (*Q. rubra*).

Its sensitivity to variations in the moisture content in leaves[21–23] makes it useful, considering that low leaf moisture is an indication of drought and some pests.[23] Detection of these variables increases NDWI's value in characterizing a variety of forest canopy changes.

1.3 *Statement of the Problem*

Careful *in situ* and laboratory observations of the unprecedented ROB damage (e.g., Ref. 3) reveal serious risk to lumber quality and other forest services to both public and extensive private forest land interests. Although aerial observer surveys were conducted by the USDA Forest Service during the outbreak, tools are needed for systematically monitoring dynamics of the oak hickory forest canopy in relationship to populations of this specific insect. Key dates of interest include low population levels in 1990, and peak outbreak population levels in 2001.[24] Repeated monitoring also implies a study of postoutbreak conditions while taking into account other forest events, such as an unprecedented January 2009 ice storm that severely damaged forest canopies across the Ozark Mountains.

Although remote sensing observations alone may provide some insights, there is a specific need in this case to compare, in conjunction with remote sensing, ROB-related *in situ* conditions after the fact. There are other forest dynamics, such as lumber activities and other driving forces behind oak mortality that are best understood through *in situ* observation. Although Wang et al.[23] examined Landsat NDWI-derived forest change in conjunction with Forest Inventory and Analysis data for the Mark Twain National Forest in Missouri, there is a need to also address ONF changes using ROB-specific field data in conjunction with postoutbreak satellite observations. Therefore, this targeted *in situ* study, combined with a multitemporal Landsat NDWI-derived change detection workflow for low, peak outbreak, and postoutbreak conditions, addressed the following questions:

1. What after the fact *in situ* characteristics are found in areas where changes are detected using Landsat NDWI derivatives from imagery acquired before and during the peak ROB outbreak (1990 to 2001)?
2. Do *in situ* data reflect variations in multiple levels of positive and negative changes detected using Landsat NDWI derivatives?
3. What new information is provided by *in situ* combined with Landsat NDWI derivatives regarding forest recovery or other changes that occurred after the outbreak?

2 Methods

2.1 *Study Area*

The ONF in Arkansas covers ~426,000 ha and extends to the southernmost portion of the Ozark Mountains. The terrain of the ONF is mountainous and rugged, with vegetation dominated by a variety of oak-hickory species interspersed with pine forest.[25] The largest contiguous portion of the ONF is the area of interest for the combined *in situ* and Landsat-derived change detection study. Targeted ONF field surveys from 48 variable radius plots measured in the summer of 2009 were collected as an *in situ* comparison.

2.2 *Remote Sensor Data*

2.2.1 *Landsat imagery*

The Landsat imagery in the NDWI change detection workflow was downloaded from the Global Land Cover Facility.[26] They were acquired by Landsat 5 TM (October 5, 1990; September 15, 2006) and Landsat 7 ETM+ (September 9, 2001). These specific dates were chosen because of the relatively low levels of cloud cover during image acquisition, and because they correspond to forest conditions before, during, and after the ROB outbreak.

The Landsat 5 TM and Landsat ETM+ imagery were orthorectified and coregistered using EarthSat's international GeoCover protocol. The NASA Stennis Space Center assessed this geometric correction protocol and reported a global root-mean-square error of ~50 m when compared with geodetic control. Since 50 m exceed the dimensions of a Landsat pixel, the question of geometric correction is warranted. However, the relative geometric fidelity of the USA imagery utilized in this study, while not reported quantitatively in the NASA assessment, is visually excellent. This can be attributed to the inclusion of a multitemporal coregistration process in the GeoCover workflow.

2.2.2 *Atmospheric correction*

Given that radiant flux is attenuated by Earth's atmosphere, the question of whether to apply atmospheric correction to satellite imagery is an important consideration in change detection applications. Some change detection approaches, such as postclassification detection, do not require atmospheric correction because the classification technique is applied in a date-specific manner. However, the atmospheric attenuation influences reflectance of biophysical measurements, and can change the values of vegetation index transformations (such as NDWI) more than 50% over thin canopy conditions.[22,27] A change detection histogram value of zero, where the histogram is based on subtraction of vegetation index images over two dates, signifies "no change" in the index (from atmospheric effects) depending on the success of the atmospheric correction.[22]

Prior to calculation of vegetation indices, atmospheric correction was applied to each Landsat image using the PCI Geomatics ATCOR-2 (atmospheric correction) module.[28] This process converts the brightness values of the raw images to percent reflectance values that are comparable over space and time. In our specific workflow, care was taken to account for changes in Landsat 5 TM radiometric calibration procedures between 1990 and 2006.[29]

2.2.3 *Normalized difference water index*

Two atmospherically corrected Landsat bands were utilized to calculate NDWI, including the NIR (band 4) and the MIR (band 5) percent reflectance. Pine-dominated stands and nonforested areas (urban regions, major roads, bodies of water) were excluded from the study using an internal Center for Advanced Spatial Technologies map derived from two Landsat 5 images collected in 2006 for both deciduous leaf-on and leaf-off conditions. This allowed further calculations to only include deciduous oak-hickory dominated forest. Atmospherically-corrected percent reflectance data for the deciduous forest canopies were then used to calculate NDWI:

$$\mathrm{NDWI} = \frac{\mathrm{NIR} - \mathrm{MIR}}{\mathrm{NIR} + \mathrm{MIR}},$$

where the NDWI is the normalized difference water index described by Gao,[21] the NIR is the near-infrared band 4 (0.76 to 0.90 μm), and the MIR is the middle-infrared band 5 (1.55 to 1.75 μm).

Pixels in the 1990 NDWI image were subtracted from corresponding pixels of the 2001 NDWI image (resulting in $\Delta\mathrm{NDWI}_{2001-1990}$), and the pixels from the 2001 NDWI image were subtracted from corresponding pixels in the 2006 image (resulting in $\Delta\mathrm{NDWI}_{2006-2001}$). These two ΔNDWI images, each representing forest canopy change between collection dates, were transformed into "peak minus low" ROB and "postoutbreak minus peak" ROB class layers (Fig. 2). These two layers are accessible online through University of Arkansas Forest Entomology's Applied Silvicultural Assessment Hazard Map.[30] A related $\Delta\mathrm{NDWI}_{2006-1990}$ image and associated class layer were also generated in order to address overall change from low ROB to aftermath recovery conditions.

Normal histograms were observed for all three ΔNDWI images, and the standard deviations of the change images were all similar as follows: 0.09 (2001 to 1990), 0.07 (2006 to 2001), and 0.08 (2006 to 1990). This can be explained by the fact that most of the forest remained intact during increased ROB activity (only certain species were affected by ROB), and multiple

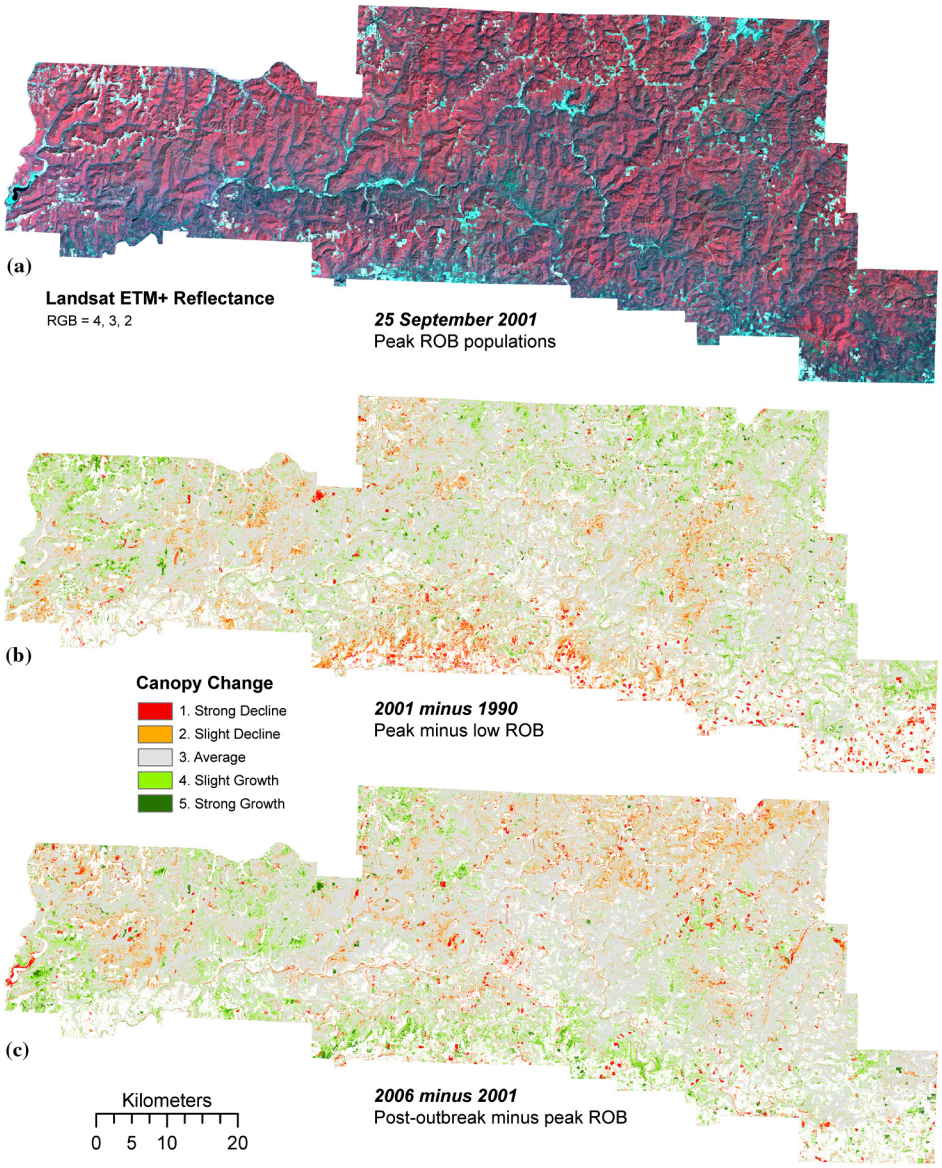

Fig. 2 (a) Landsat 7 ETM+ reflectance imagery (RGB = 4, 3, 2) collected 25 Sep 2001 during peak red oak borer (ROB) conditions; (b) and (c) Landsat 7 ETM+ normalized difference vegetation index-derived canopy change (ΔNDWI) maps for two epochs including "peak minus low" ROB and "postoutbreak minus peak" ROB.

comparable dynamics were present in all three epochs (e.g., selective timber harvests, clear cutting, ROB activity, forest regrowth, etc.). In contrast, histogram means varied as follows: −0.19 (2001 to 1990), 0.21 (2006 to 2001), and 0.02 (2006 to 1990). If exactly comparable source imagery were available, it would make sense for zero ΔNDWI values (in normal histograms) to represent zero change. However, no claim is made that the ATCOR-2 workflow perfectly removes the effects of atmospheric attenuation. Furthermore, variation in instantaneous leaf moisture content and exact phenological conditions were not accounted for (although all images were selected based on near anniversary dates). Given the question of exact comparability of the Landsat images, zero ΔNDWI values were assumed to possibly represent some change. However, if the peak of a normal ΔNDWI histogram represents little or no change overall (when most of the forest remains intact), then the histogram average is a better approximation of "no change." Based on this logic and the fact that all three histograms had similar standard deviations, we utilized statistical (standard deviations from the mean) thresholds to rapidly identify five categorical changes (Fig. 2).

Each ΔNDWI image was first subtracted by its mean (μ) and then divided by its standard deviation ($\Delta NDWI_{\sigma\mu}$). This approach is very similar to that used for the Mark Twain National Forest by Wang et al.[23] who, instead of subtracting the mean, applied a histogram match process for a similar purpose. In our resulting $\Delta NDWI_{\sigma\mu}$ image, the mean value represents the average change that occurred and is a good approximation of no change given the aforementioned histogram properties. The $\Delta NDWI_{\sigma\mu}$ values < -1 (in σ units) were labeled decline, and values >1 were labeled growth. These categories were used to address *in situ* characteristics identified in Landsat-derived change categories from a low population to peak ROB activity (1990 to 2001). Growth and decline categories were further subdivided into slight decline ($-2 < \Delta NDWI_{\sigma\mu} < -1$), strong decline ($\Delta NDWI_{\sigma\mu} < -2$), slight growth ($1 < \Delta NDWI_{\sigma\mu} < 2$), and strong growth ($\Delta NDWI_{\sigma\mu} > 2$). These subcategories were used to address whether *in situ* data reflect variations in multiple levels of positive and negative changes detected using Landsat NDWI derivatives. The five categories were also used to address new information provided by *in situ* combined with Landsat NDWI derivatives regarding forest change during the postoutbreak aftermath (2001 to 2006).

2.3 *In Situ Data Collection*

Forty-eight variable radius point plots were established and vegetation surveys were conducted at each plot. Using ArcGIS, plots were selected randomly on public land within a 400-m buffer from forest roads. The buffer allowed reasonable access over a broad area in rugged terrain. Within each plot, trees with a diameter at breast height (DBH) $\geq$5 cm were sampled using a wedge prism with a basal area factor of 1 $m^2\,ha^{-1}$. The prism allows the surveyor to take a sample of a stand's population by tallying all trees that are greater in size than the prism's projected angle. Plot basal area and stem densities were calculated in the standard manner.[31] Species diversity was calculated using the Shannon–Wiener index (H'), which shows the relationship between species richness or the number of species in a community, and species evenness or the relative abundance of the species.[32]

Five *Q. rubra* trees were chosen from each of 42 of the plots for increment core extraction to determine stand age and growth patterns. For every *Q. rubra* in each of these same plots, a crown class index (CCI) was recorded. Four classes were identified based on the percentage of crown dieback: CCI 1 (1% to 33%), CCI 2 (34% to 66%), CCI 3 (66% to 99%), CCI 4 (100% or dead crown).

2.4 *Increment Core Processing*

Tree cores were crossdated using standard techniques.[33,34] A Velmex "TA" system[35] and MeasureJ2X software[36] were used to measure tree-ring widths to the nearest 0.001 mm.

For both growth and decline plots, raw ring-width measurements from 1991 to 2008 were standardized by dividing them by the arithmetic mean ring-width (e.g., average growth) over each tree's lifetime. Mean standardized annual growth rate was then calculated for each tree core (66 cores from decline plots and 40 cores from growth plots) during two time periods (1991 to 2000 and 2001 to 2008). The effects of time period and plot type, and their interactions on standardized growth rate were analyzed with two-way analysis of variance.[37]

2.5 *Machine Learning Decision Tree Classification*

In situ plot data were analyzed using the C5.0 machine learning decision tree algorithm,[22,38] recently made available by Rulequest Research[39] under a GNU General Public License. C5.0 was configured to produce classification rule sets, where each rule may contain one or more if-then statements that in combination predict a specific class (e.g., strong growth) at a given probability (e.g., 87%). A secondary configuration caused C5.0 to winnow attributes determined by the algorithm to contain low information content relative to prediction of the five target classes (strong decline, slight decline, average, slight growth, and strong growth). Three distinct C5.0 rule sets were constructed (Table 1), all based on five variables from *in situ* data: mean age of *Q. rubra*, mean DBH, density, basal area, and species diversity. The first rule set was developed to predict the five categories associated with Landsat NDWI-derived change from 1990 to

Table 1 Three distinct C5.0 rule sets were constructed. Available source attributes [e.g., mean diameter at breast height (DBH)] were the same for all rule sets but level of detail in change categories, time period, and red oak borer (ROB) status were varied. The specific research question (as identified in 1.4) addressed by each rule set is also given.

C5.0 rule set	Source attributes	Change categories predicted	Time period	ROB activity	Research question addressed
1	Mean age Density	Strong decline Slight decline	1990 to 2001	Low to outbreak	2
2	Basal area Species diversity Mean DBH	Average Slight growth Strong growth	2001 to 2006	Peak to low	2, 3
3		Decline Average Growth	1990 to 2001	Low to outbreak	2

2001 (low to peak ROB). The second rule set was structured similarly except that it was applied to the years 2001 to 2006 (peak ROB to postoutbreak).

The third rule set predicts three broad ΔNDWI-related change categories pertaining to the years 1990 to 2001: decline ($\Delta\text{NDWI}_{\sigma\mu} < -1$), average ($\Delta\text{NDWI}_{\sigma\mu} > 2$, and growth (positive changes $> \sigma$). This rule set was devised to compare the effectiveness of broader change categories with those having more variation including change categories in rule sets 1 and 2 (Table 1). Interpretation of the detailed rules developed in these two classifiers, as well as their effectiveness, addressed how well the *in situ* data reflects the Landsat NDWI-derived change detection.

3 Results

Certain differences and similarities between general growth and decline categories were noted during initial observations. Trees found in areas of growth were generally smaller and younger, while trees in areas of decline were larger and older (Fig. 3). Growth stands were denser than decline stands, and decline stands had a higher basal area. Growth plots were populated with occasional large trees, but were mostly composed of root sprouts from numerous cut stumps, while decline plots consisted of mature and over-mature trees, often with a dense understory and canopy gaps (Fig. 3). Within decline plots, 40% of trees measured were *Q. rubra*, and nearly a quarter of these were dead. Crown conditions of *Q. rubra* varied, with CCI 2 and CCI 3 sharing the highest frequency (Table 2). In contrast, species diversity did not differ much between plot types (Table 3). Also, there were no significant differences in standardized annual growth rate by plot type or by time period ($P > 0.05$; Fig. 4).

The rule sets and supporting documentation generated by C5.0 provide a variety of information related to the *in situ* data that is useful for predicting Landsat-derived change categories (Table 4). Rules with if-then statements were only generated in the first and third rule sets which both pertained to the years 1990 to 2001 ROB infestation period. From 2001 to 2006, most of the *in situ* plots (31 out of 48) were associated with the middle (average) category approximating little or no change. In this instance, C5.0 generated a rule to simply predict that average change category. However, this approach is only 64.6% accurate in predicting the data used in the classification training process (see C5.0 rule set 2 in Table 4).

Aggregation of the Landsat NDWI-derived change categories is associated with some improvement in accuracy (from 81.2% to 85.4%). For the low to peak ROB (infestation) period from 1990 to 2001, mean DBH was estimated to be the most important *in situ* variable (64% in the first rule set and 100% in the third rule set). Other variables were found to be relatively less important (<1%) including during the peak to postoutbreak (recovery) period from 2001 to 2006. In the development of each rule set, at least 40% (2 out of 5) attributes were winnowed by C5.0 or judged to not contain relevant predictive ability. Basal area was not included in any of the rule sets.

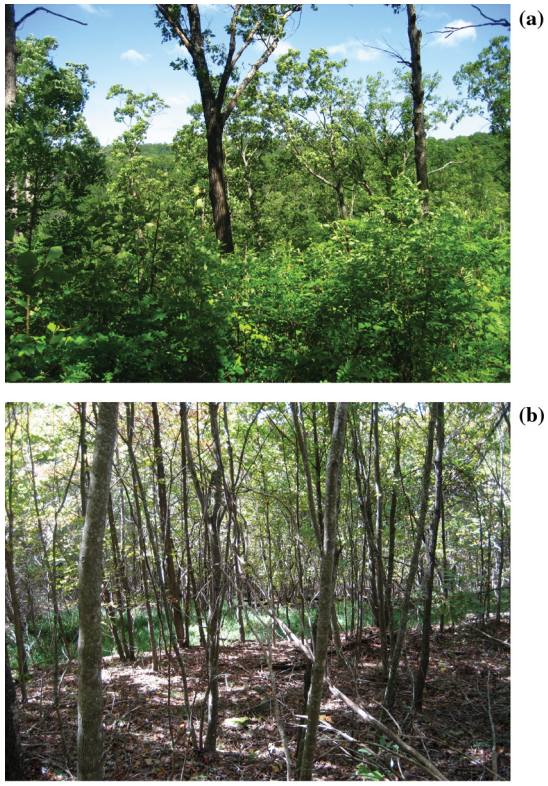

Fig. 3 (a) Decline plot with dense understory, canopy gaps, and larger trees with varying levels of crown dieback, and (b) growth plot with clear understory, smaller trees, and no evidence of crown dieback.

4 Discussion

Although the *in situ* data collection was time and resource intensive, it proved useful for addressing (~8 years after peak ROB activity) a number of characteristics associated with Landsat NDWI-derived growth and decline areas. This includes, for example, the frequency of stressed or dead *Q. rubra* in decline plots. Of course, it would be difficult to exactly compare crown conditions recorded in the year 2009 field study with those at the time the 2001 satellite image was acquired. However, oaks tend to grow slowly when stressed, and can take a long

Table 2 Mean proportions of *Quercus rubra* within each crown class index within general Landsat normalized difference water index (NDWI)-derived categories.

Landsat NDWI-derived category	CCI 1 (1% to 33% dieback)	CCI 2 (34% to 66% dieback)	CCI 3 (67% to 99% dieback)	CCI 4 (100% dead)
Growth	0.72	0.09	0.09	0.14
Decline	0.18	0.36	0.36	0.09

Table 3 Mean values of variables calculated from *in situ* data for growth and decline within general Landsat NDWI-derived categories.

Landsat NDWI-derived category	DBH (cm)	Age (y)	Density (trees/ha)	Basal area (m^2/ha)	H'
Growth	16.6	26.2	1516.21	18.52	1.32
Decline	31.4	87.2	524.13	14.07	1.35

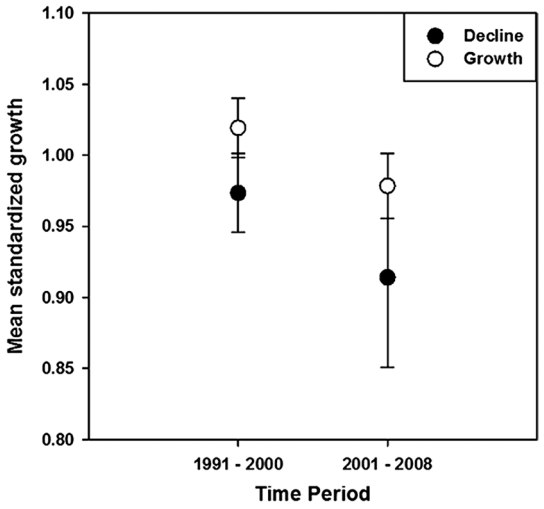

Fig. 4 Mean standardized annual growth rate for *Q. rubra* in decline and growth plots, grouped by time periods coinciding with $\Delta NDWI_{2001-1990}$ and $\Delta NDWI_{2006-2001}$.

while to die,[4,40,41] so *in situ* decline observed in 2009 was likely indicative of decline that was occurring in 2001.

The bark of dead *Q. rubra* was often partially or completely decomposed, and the presence of the ROB heartwood galleries was common [Fig. 1(b)]. Such qualitative observations support the hypothesis that ROB outbreak played a key role in the decline of *Q. rubra* in decline plots. A few decline plots contained no evidence of the ROB or oak decline and mortality. There were instances of tree thinning in which a few trees were harvested and many were left. These were likely identified because of biomass decreases due to the recent partial removal of the canopy. The Landsat NDWI-derived change maps (Fig. 2) would not distinguish between this type of thinning and ROB-related dieback on a pixel by pixel basis. Published expert rules involving slope, aspect, elevation, insolation, etc. have been reported for various levels of the ROB hazard.[30,42] However, this study offers a simple and cost effective Landsat-based linkage that can identify probable areas of either (a) thinning or (b) crown dieback; this information can therefore be used to augment the landscape analysis work and can lead to more effective ROB hazard prediction.

Tree-ring data were useful for showing the stand age differences between decline and growth plots, but were not as useful for relating growth patterns to plot types. Radial growth during both time periods was essentially average for those trees when they had lost/gained leaf area. There were, however, clear differences between the growth and decline plots in nonstandardized raw ring-widths. These differences were likely due to the earlier developmental stage of trees in growth plots; they grew much faster than those in decline plots during both time periods.

The NDWI-derived change detection was successful in identifying forest regeneration, and showed that it was not in conjunction ROB-induced oak decline. The regeneration detected was

Table 4 Number of rules with if-then statements, default class (for use in cases where no if-then statements apply), estimated importance of individual attributes, and training data prediction accuracy associated with the three C5.0 rule sets.

C5.0 rule set	Time period	Number of production rules	Default class	Estimated importance of attributes	Training data prediction accuracy (%)
1	1990 to 2001	6	Strong growth	64% Mean DBH <1% Density	81.2
2	2001 to 2006	0	Average	<1% Species diversity	64.6
3	1990 to 2001	3	Growth	100% Mean DBH <1% Mean age <1% Density	85.4

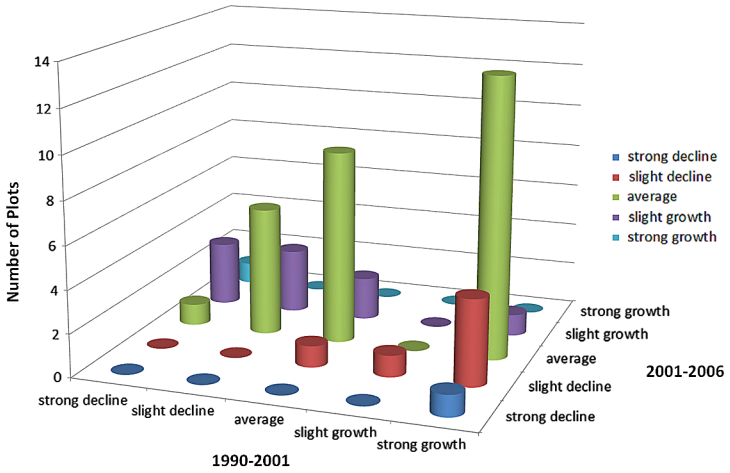

Fig. 5 Plot category migration (as identified using Landsat NDWI-derived change detection) from the 1990 to 2001 ROB infestation period to the 2001 to 2006 postoutbreak period.

the result of anthropogenic influences in these forest stands, as they were found in areas in which most trees had been harvested. The growth areas delineated by $\Delta NDWI_{2001-1990}$ most likely resulted from sprout and seedling regeneration that occurred in these stands after large scale cuts.[43,44]

The careful application of remote sensing to detect regeneration in stands is important within the context of oak decline that older forest stands have experienced. Species composition and evenness (H') of growth plots were similar to decline plots, and plot types were for the most part even-aged. This suggests that in 60 or 70 years from now, when the young growth plot trees reach maturity, they will be stands that resemble the current declining ones. These stands could be considered potential ROB hazard areas in the future.

The C5.0 analysis support provided insight into the questions of change variation and forest recover (Table 4). Regarding how well the Landsat-derived record reflects *in situ* variations, it is clear from the three rule sets produced that the *in situ*-Landsat relationship is markedly stronger during the 1990 to 2001 ROB infestation period (81.2% to 85.4%) than during the 2001 to 2006 postoutbreak, low level period (64.6%). This suggests that growth conditions observed *in situ* are less recognizable using 30×30 m satellite imagery than are decline conditions. This may be related to the complexity of discriminating forest structure using multispectral information.[45]

The range of 81.2% to 85.4% predictive ability between five and three NDWI-derived change categories suggests that historical Landsat data is suitable for a five-category assessment. This 4% decrease is not a major loss in accuracy when additional categorical detail may provide useful information to forest managers.

Addressing the final research question regarding *in situ* and Landsat data with respect to the 2001 to 2006 period of low ROB density, the data show a marked increase in the number of average change categories, with strong decline and slight decline plots also falling into slight growth categories (Fig. 5). *Q. rubra* was still in decline after the ROB outbreak subsided, and 2006 was a drought year, suggesting that the migration of decline categories to growth categories was due to detection of flourishing undergrowth as canopy gaps were created from the continued tree mortality.[46]

The process of monitoring ROB-related canopy changes using a satellite platform with a nominal spatial resolution of 30×30 m can be improved through incorporation of additional ancillary and *in situ* data as well as additional satellite imagery, both past and future. Although historical Landsat data has been shown to be cost-effective and efficient when used to detect forest canopy change, there may be a need for additional categorical detail (e.g., an increase from five to seven categories of change/no change) in order to better characterize ROB hazard. Rather than using standard deviations, future research could maximize the number of useful categories based on the inherent spatial and radiometric information content in the data (e.g., through object-based image analysis and clustering techniques). Given its dramatically improved radiometric resolution as well as additional and refined spectral bands, Landsat 8

promises to offer an increase in the ability to detect future subtle canopy changes. If developed as a monitoring resource, the application of Landsat 8 will already be reined as *in situ* and other observations identify possible future ROB infestations.

5 Conclusions

A forest canopy change application of a Landsat TM/ETM+ NDWI, compared with *in situ* forest observations, revealed previously unknown locations of disturbed forest stands that consistently showed signs of past ROB infestation. Regenerating forest stands were also found with stump sprouts close to the same age as the first satellite image used for change detection. This indicates that these areas were heavily cut, and the detected regeneration is a response to anthropogenic influences rather than ROB-related oak decline. Decadal application of change detection revealed forest stands that experienced disturbance, and young stands that may experience forest decline in the future when their trees become senescent. The DBH was found to be an important predictor of the ROB hazard and the easiest measurement to make *in situ*. Incorporation of historical and future Landsat data using different time periods and thresholds can refine the process of ROB-related oak-hickory forest monitoring and further improve landscape prediction of the ROB hazard.

Acknowledgments

This study was supported by the USDA Forest Service Southern Research Station "Applied Silvicultural Assessment of Upland Oak-Hickory Forests and the Red Oak Borer in the Ozark and Ouachita Mountains of Arkansas" and by USGS award number 08HQGR0157 "America View: A National Remote Sensing Consortium." The authors directed the design, analysis, and preparation of published material and data.

References

1. F. M. Stephen, V. B. Salisbury, and F. L. Oliveria, "Red oak borer, *Enaphalodes rufulus* (Coleoptera: Cerambycidae), in the Ozark Mountains of Arkansas, U.S.A.: an unexpected and remarkable forest disturbance," *Integr. Pest Manage. Rev.* **6**(3–4), 247–252 (2001), http://dx.doi.org/10.1023/A:1025779520102.
2. M. K. Fierke, M. B. Kelley, and F. M. Stephen, "Site and stand variables influencing red oak borer, *Enaphalodes rufulus* (Coleoptera: Cerambycidae), population densities and tree mortality," *For. Ecol. Manage.* **247**(1–3), 227–236 (2007), http://dx.doi.org/10.1016/j.foreco.2007.04.051.
3. M. K. Fierke et al., "Development and comparison of intensive and extensive sampling methods and preliminary within-tree population estimates of red oak borer (Coleoptera: Cerambycidae) in the Ozark Mountains of Arkansas," *Environ. Entomol.* **34**(1), 184–192 (2005), http://dx.doi.org/10.1603/0046-225X-34.1.184.
4. L. J. Haavik and F. M. Stephen, "Stand and individual tree characteristics associated with *Enaphalodes rufulus* (Haldeman) (Coleoptera: Cerambycidae) infestations within the Ozark and Ouachita National Forests," *For. Ecol. Manage.* **259**(10), 1938–1945 (2010), http://dx.doi.org/10.1016/j.foreco.2010.02.005.
5. J. J. Riggins, L. D. Galligan, and F. M. Stephen, "Rise and fall of red oak borer (Coleoptera: Cerambycidae) in the Ozark Mountains of Arkansas, USA," *Fla. Entomol.* **92**(3), 426–433 (2009), http://dx.doi.org/10.1653/024.092.0303.
6. C. J. Hay, "Survival and mortality of red oak borer larvae on black, scarlet, and northern red oak in eastern Kentucky," *Ann. Entomol. Soc. Am.* **67**(6), 981–986 (1974).
7. M. K. Fierke et al., "A rapid estimation procedure for within-tree populations of red oak borer (Coleoptera: Cerambycidae)," *For. Ecol. Manag.* **215**(1–3), 163–168 (2005), http://dx.doi.org/10.1016/j.foreco.2005.05.009.
8. D. A. Starkey et al., "Oak decline and red oak borer in the interior highlands of Arkansas and Missouri: natural phenomena, severe occurrences," in *Upland Oak ecology symposium:*

history, current conditions, and sustainability, pp. 217–222, M. A. Spetich, Ed., Fayetteville, Arkansas, Gen. Tech. Rep. SRS-73, U.S. Department of Agriculture, Forest Service, Southern Research Station, Asheville, NC (2004).
9. M. K. Fierke, "Distribution and abundance, stand and site conditions, host selection and oak defenses associated with a red oak borer (Coleoptera: Cerambycidae) outbreak in the Ozark National Forest, Arkansas," Dissertation, Department of Entomology, University of Arkansas, Fayetteville (2006).
10. J. M. Guldin et al., "Ground truth assessments of forests affected by oak decline and red oak borer in the interior highlands of Arkansas, Oklahoma, and Missouri: Preliminary results from overstory analysis," in *Proc. 13th Bienn. South. Silvicultural Res. Conf.*, pp. 415–419, K. F. Connor, Ed., Asheville, North Carolina (2006).
11. E. Heitzman et al., "Changes in forest structure associated with oak decline in severely impacted areas of northern Arkansas," *South. J. Appl. For.* **31**(1), 17–22 (2007).
12. E. Heitzman, "Effects of oak decline on species composition in a northern Arkansas forest," *South. J. Appl. For.* **27**(4), 264–268 (2003).
13. D. E. Donley and E. Rast, "Vertical distribution of the red oak borer, *Enaphalodes rufulus* (Coleoptera: Cerambycidae) in red oak," *Environ. Entomol.* **13**(1), 41–44 (1984).
14. R. H. Wynne and D. B. Carter, "Will remote sensing live up to its promise for forest management?," *J. For.* **95**(10), 23–36 (1997).
15. K. Lim et al., "LiDAR remote sensing of forest structure," *Prog. Phys. Geogr.* **27**(1), 88–106 (2003), http://dx.doi.org/10.1191/0309133303pp360ra.
16. P. R. Coppin and M. E. Bauer, "Digital change detection in forest ecosystems with remote sensing imagery," *Remote Sens. Rev.* **13**(3–4), 207–234 (1996), http://dx.doi.org/10.1080/02757259609532305.
17. J. R. Jensen," *Remote Sensing of the Environment: An Earth Resource Perspective*," Prentice Hall, Upper Saddle River, New Jersey (2000).
18. P. R. Coppin et al., "Digital change detection methods in ecosystem monitoring: a review," *Int. J. Remote Sens.* **25**(9), 1565–1596 (2004), http://dx.doi.org/10.1080/0143116031000101675.
19. C. E. Woodcock et al., "Free access to Landsat imagery," *Science* **320**(5879), 1011 (2008), http://dx.doi.org/10.1126/science.320.5879.1011a.
20. USGS, "USGS global visualization viewer," http://glovis.usgs.gov/ accessed (August 9 2013).
21. B. C. Gao, "NDWI—A normalized difference water index for remote sensing of vegetation liquid water from space," *Remote Sens. Environ.* **58**(3), 257–266 (1996), http://dx.doi.org/10.1016/S0034-4257(96)00067-3.
22. J. R. Jensen, *Introductory Digital Image Processing: A Remote Sensing Perspective*, 3rd ed., Prentice Hall, Upper Saddle River, New Jersey (2005).
23. C. Wang, Z. Lu, and T. Haithcoat, "Using Landsat images to detect oak decline in the Mark Twain National Forest, Ozark Highlands," *For. Ecol. Manage.* **240**(1–3), 70–78 (2007), http://dx.doi.org/10.1016/j.foreco.2006.12.007.
24. L. J. Haavik and F. M. Stephen, "Historical dynamics of a native cerambycid, *Enaphalodes rufulus*, in relation to climate in the Ozark and Ouachita Mountains of Arkansas," *Ecol. Entomol.* **35**(6), 673–683 (2010), http://dx.doi.org/10.1111/een.2010.35.issue-6.
25. R. D. Soucy, E. Heitzman, and M. A. Spetich, "The establishment and development of oak forests in the Ozark Mountains of Arkansas," *Can. J. For. Res.* **35**(8), 1790–1797 (2005), http://dx.doi.org/10.1139/x05-104.
26. Global Land Cover Facility, "GLCF Data Guides," http://www.landcover.org/library/guide/ (24 September 2013).
27. C. Song et al., "Classification and change detection using Landsat TM data: When and how to correct atmospheric effects," *Remote Sens. Environ.* **75**(2), 230–244 (2001), http://dx.doi.org/10.1016/S0034-4257(00)00169-3.
28. PCI Geomatics, "Geomatica 9," Alexandria, Virginia (2003).
29. G. Chander and B. Markham, "Revised Landsat-5 TM radiometric calibration procedures and postcalibration dynamic ranges," *IEEE Trans. Geosci. Remote Sens.* **41**(11), 2674–2677 (2003), http://dx.doi.org/10.1109/TGRS.2003.818464.

30. J. A. Tullis et al., "Applied Silvicultural Assessment (ASA) Hazard Map" http://asa.cast.uark.edu/hazmap/, 10 August 2012 (24 September 2013).
31. B. Husch, T. W. Beers, and J. A. Kershaw, *Forest Mensuration*, 4th ed., John Wiley and Sons, Hoboken, New Jersey (2003).
32. C. E. Shannon, "A mathematical theory of communication," *Bell Syst. Tech. J.* **27**(3), 379–423 (1948), http://dx.doi.org/10.1002/bltj.1948.27.issue-3.
33. A. E. Douglass, "Crossdating in dendrochronology," *J. For.* **39**(10), 825–831 (1941).
34. M. A. Stokes and T. L. Smiley, *An Introduction to Tree-Ring Dating*, The University of Arizona Press, Tucson, Arizona (1996).
35. Velmex, Inc., "*The Velmex 'TA' System for Research and Non-contact Measurement Analysis*," Velmex, Inc., Bloomfield, New York (2008).
36. VoorTech Consulting, *MeasureJ2X*, Holderness, New Hampshire (2007).
37. Systat Software, "*Sigmaplot 11.0*," San Jose, California, http://www.systat.com/ (2008).
38. J. R. Quinlan, *C4.5: Programs for Machine Learning*, Morgan Kaufman Publishers, San Mateo, California (1993).
39. Rulequest Research, "Data Mining Tools See5 and C5.0," http://www.rulequest.com (1 December 2012).
40. J. P. Dwyer, B. E. Cutter, and J. J. Wetteroff, "A dendrochronological study of black and scarlet oak decline in the Missouri Ozarks," *For. Ecol. Manage.* **75**(1–3), 69–75 (1995), http://dx.doi.org/10.1016/0378-1127(95)03537-K.
41. M. A. Jenkins and S. G. Pallardy, "The influence of drought on red oak group species growth and mortality in the Missouri Ozarks," *Can. J. For. Res.* **25**, 1119–1127 (1995), http://dx.doi.org/10.1139/x95-124.
42. L. D. Aquino, J. A. Tullis, and F. M. Stephen, "Modeling red oak borer, *Enaphalodes rufulus* (Haldeman), damage using in situ and ancillary landscape data," *For. Ecol. Manage.* **255**(3–4), 931–939 (2008), http://dx.doi.org/10.1016/j.foreco.2007.10.011.
43. C. J. Atwood, T. R. Fox, and D. L. Loftis, "Effects of alternative silviculture on stump sprouting in the southern Appalachians," *For. Ecol. Manage.* **257**(4), 1305–1313 (2009), http://dx.doi.org/10.1016/j.foreco.2008.11.028.
44. R. C. Morrissey et al., "Competitive success of natural oak regeneration in clearcuts during the stem exclusion stage," *Can. J. For. Res.* **38**(6), 1419–1430 (2008), http://dx.doi.org/10.1139/X08-018.
45. J. M. Defibaugh y Chávez and J. A. Tullis, "Deciduous forest structure estimated with LiDAR-optimized spectral remote sensing," *Remote Sens.* **5**(1), 155–182 (2013), http://dx.doi.org/10.3390/rs5010155.
46. L. J. Haavik et al., "Oak decline and red oak borer outbreak: Impact in upland oak-hickory forests of Arkansas, USA," *Forestry* **85**(3), 341–352 (2012), http://dx.doi.org/10.1093/forestry/cps032.

Biographies of the authors are not available.